Published in final edited form as:
Science. 2013 September 27; 341(6153): . doi:10.1126/science.1240636.

Circadian gene Bmal1 regulates diurnal oscillations of Ly6C^{hi} inflammatory monocytes

Khoa D. Nguyen[1,2], **Sarah J. Fentress**[3], **Yifu Qiu**[1], **Karen Yun**[1], **Jeffery S. Cox**[3], and **Ajay Chawla**[1,4]

[1]Cardiovascular Research Institute, University of California San Francisco, 94158-9001, USA

[2]Immunology Program, Stanford University, CA 94305, USA

[3]Department of Microbiology & Immunology, University of California, San Francisco, 94158-9001, USA

[4]Departments of Physiology and Medicine, University of California San Francisco, 94158-9001, USA

Abstract

Circadian clocks have evolved to regulate physiologic and behavioral rhythms in anticipation of changes in the environment. Although the molecular clock is present in innate immune cells, its role in monocyte homeostasis remains unknown. Here, we report that Ly6C^{hi} inflammatory monocytes exhibit diurnal variation, which controls their trafficking to sites of inflammation. This cyclic pattern of trafficking confers protection against *Listeria monocytogenes* and is regulated by the repressive activity of the circadian gene BMAL1. Accordingly, myeloid cell-specific deletion of BMAL1 induces expression of monocyte-attracting chemokines and disrupts rhythmic cycling of Ly6C^{hi} monocytes, predisposing mice to development of pathologies associated with acute and chronic inflammation. These findings have unveiled a critical role for BMAL1 in controlling the diurnal rhythms in Ly6C^{hi} monocyte numbers.

Introduction

The circadian clock is a timekeeping system that allows organisms to adapt their physiological and behavioral rhythms to anticipatory changes in their environment (1, 2). In mammals, the circadian timing system has a hierarchical architecture, consisting of the light responsive central clock in the suprachiasmatic nuclei and the peripheral clocks that are present in virtually all cells of the body (3). While the central clock entrains and synchronizes the peripheral clocks with the day-night cycle, the peripheral clocks regulate tissue-specific programs in an anticipatory manner. Although the peripheral clock has been identified in macrophages (4-9), its role in anticipatory immune responses remains poorly understood.

In simple terms, the inflammatory response can be expressed as a product of inducible gene expression in an innate cell multiplied by the number of infiltrating innate cells. When examined from this viewpoint, circadian oscillations could potentially regulate inflammatory responses by modulating rhythmic expression of inflammatory genes in tissue macrophages or by controlling rhythmic trafficking of Ly6C^{hi} inflammatory monocytes (10, 11). Because the cumulative cost incurred by rhythmic expression of inflammatory genes is likely to be high (in terms of tissue inflammation and damage), we postulated that rhythmic mobilization

The authors declare that they have no competing financial interests.

of Ly6C^{hi} monocytes provides a better means of mounting anticipatory inflammatory responses. In this scenario, the rhythmic mobilization of Ly6C^{hi} monocytes would fortify the host's innate immune defences in anticipation of environmental challenges, a process we term “anticipatory inflammation.”

Results

Diurnal oscillations and trafficking of Ly6C^{hi} monocytes

To investigate this hypothesis, we examined whether blood monocytes exhibited diurnal variation in expression of clock genes. Analysis of monocytes obtained from mice kept under 12 hr light-dark cycle revealed rhythmic expression of mRNA encoded by the clock gene Bmal1 (*Arntl*), whose oscillation was anti-phasic to its two target genes *Nr1d1* and *Dbp* (Fig. 1A). A similar rhythm was observed for luciferase protein in monocytes derived from *Per2^{Luc}* knock-in mice (12), which express PERIOD2 as a luciferase fusion protein (fig S1A). Furthermore, serum synchronization of THP-1 cells, a human monocytic cell line, revealed 24 hr oscillation of clock genes under constant culture conditions (fig. S1B). Together, these data demonstrate that blood monocytes exhibit diurnal variation in clock genes, which might impart rhythmicity to their functions.

Recent studies have demonstrated rhythmic trafficking of immune cells into tissues (6, 8), prompting us to ask whether monocyte frequency in the three major reservoirs (blood, spleen, and bone marrow) also varies in a diurnal manner. Indeed, between the peak and nadir Zeitgeber time (ZT, where ZT0 refers to lights on and ZT12 refers to lights off), there was ~2-fold difference in the total number of monocytes present in blood and spleen (fig. S2, S3A, B) with bone marrow displaying a reciprocal diurnal rhythm (fig. S3C).

We next examined whether the observed oscillations in total monocytes resulted from rhythmic changes in Ly6C^{hi} (inflammatory) or Ly6C^{low} (patrolling) monocytes (13, 14). The peak and nadir of Ly6C^{hi} monocytes in blood and spleen mirrored the cyclic pattern of total monocytes in these reservoirs (Fig. 1B, C and fig. S3A, B), whereas Ly6C^{low} monocytes did not display strong oscillatory behavior in blood or spleen (fig. S3D, E). Moreover, the expression of *Ccr2* mRNA in monocytes did not correlate with Ly6C^{hi} monocyte numbers in blood (fig. S3F). Since Ly6C^{hi} monocytes are recruited to sites of inflammation (15, 16), we investigated the relationship between diurnal variations in Ly6C^{hi} monocyte numbers and monocyte-driven inflammation using the thioglycollate model of sterile peritonitis (17). The numbers of Ly6C^{hi} monocytes recruited to the inflamed peritoneum at ZT8 were ~3-fold higher than at ZT0 (Fig. 1D), which resulted in ~3-3.5-fold higher inflammation, as quantified by the release of interleukin (IL)1β and IL6 (Fig. 1E and fig. S3G). On a per cell basis, expression of IL1 and IL6 did not exhibit diurnal oscillations (fig. S3H, I), suggesting that diurnal variation in Ly6C^{hi} monocyte numbers dictates the magnitude of the innate inflammatory response. Moreover, monocyte-attracting chemokines CCL2 and CCL8, whose concentrations were higher (~2-3-fold) in the inflamed peritoneum at ZT8 (fig. S3J, K), were primarily secreted by recruited monocytes and resident macrophages but not neutrophils (fig. S3L).

Diurnal rhythms of Ly6C^{hi} monocytes during *L. monocytogenes* infection

Ly6C^{hi} monocytes provide the first line defense against *L. monocytogenes* (18), leading us to posit that anticipatory oscillations in Ly6C^{hi} monocyte numbers might modulate innate responses to infection. To investigate this hypothesis, C57BL/6J mice were intraperitoneally infected with *L. monocytogenes* at ZT0 or ZT8. Two days post infection (dpi), the peritoneum, spleen, and liver of mice infected at ZT8 had significantly fewer bacteria than those infected at ZT0 (Fig. 2A-C). Improved bacterial clearance at ZT8 was associated with

~2.2-3.8-fold higher numbers of TNF (tumor necrosis factor)/iNOS (inducible nitric oxide synthase)-producing (Tip)-dendritic cells (DCs), which differentiate from Ly6C^{hi} monocytes to control the growth of this pathogen (Fig. 2D-F, fig. S4) (19). Moreover, serum, and to an even greater extent, peritoneum concentrations of chemokines and cytokines necessary for the mobilization and activation of Ly6C^{hi} monocytes were much higher at ZT8 than at ZT0 (fig. S5A and Fig. 2G). This was associated with higher recruitment of Ly6C^{hi} monocytes but not neutrophils to the peritoneum (fig. S5B-C), findings that are consistent with previous observations that neutrophils are dispensable for defense against *L. monocytogenes* (20).

While Ly6C^{hi} monocytes and Tip-DCs limit bacterial growth during the early phase of infection, efficient clearance of *L. monocytogenes* requires adaptive immunity (18), prompting us to investigate the activation of adaptive immunity 6dpi. Although the peritoneal cavity was below the limit of detection, mice inoculated at ZT8 continued to demonstrate enhanced clearance of *L. monocytogenes* in secondary sites, such as the liver (fig. S5D). In contrast, bacterial burden in the spleen was not significantly different between mice inoculated at ZT0 and ZT8, especially after normalization for spleen size (fig. S5E-G). Infection at ZT8 resulted in stronger adaptive immune response in the spleen and liver, as evidenced by ~3-4.5-fold higher numbers of interferon-γ (IFNγ) producing CD4^{+} and CD8^{+} T cells at ZT8 (fig. S4 and S5H, I). Tip-DCs were also more numerous in spleen and liver, but not the peritoneum, 6 dpi (fig. S5J-L).

Infection with a high inoculum of pathogens often results in over activation of the immune system, causing systemic inflammation and death (11). Because previous studies have demonstrated circadian influence on sepsis-induced mortality (8, 21, 22), we investigated whether the host response to infection with a higher dose of *L. monocytogenes* might exhibit similar diurnal variation. Intraperitoneal infection of mice with 1×10^{7} *L. monocytogenes* resulted in significantly higher mortality rate at ZT8 than at ZT0 (Fig. 2H). This increase in mortality was not associated with a higher bacterial burden (fig. S6A-C), but rather with an enhanced inflammatory response (Fig. 2I). These results demonstrate that the host response to *L. monocytogenes* exhibits diurnal rhythms that parallel the rhythms of Ly6C^{hi} monocytes.

BMAL1 regulates rhythmic oscillations of Ly6C^{hi} monocytes

To determine whether clock genes in monocytes regulate their diurnal rhythms, we generated myeloid-specific Bmal1 knockout mice using *Arntl*$^{LoxP/LoxP}$ and *Lyz2Cre* mice (designated *Arntl*$^{LoxP/LoxP}$*Lyz2*^{Cre}) (23). Immunoblot analysis confirmed loss of BMAL1 protein in blood monocytes of *Arntl*$^{LoxP/LoxP}$*Lyz2*^{Cre} mice (fig. S7A). Quantitative RT-PCR analysis of mRNAs provided further verification that diurnal variations of core clock genes, including *Arntl* and *Nr1d1*, were abolished in blood monocytes of *Arntl*$^{LoxP/LoxP}$*Lyz2*^{Cre} mice (fig. S7B and Fig. 3A). Remarkably, the disruption of BMAL1 expression in myeloid cells was sufficient to impair the diurnal variations in Ly6C^{hi} monocyte numbers in blood, spleen, and bone marrow (Fig. 3B-D). The normal diurnal rhythm of total monocytes was similarly disrupted in the blood and spleens of *Arntl*$^{LoxP/LoxP}$*Lyz2*^{Cre} mice (fig. S7C, D). In contrast, we failed to detect rhythmic changes in the numbers of Ly6C^{low} monocytes (fig. S7E, F) and neutrophils (fig. S7G-H) in control (*Arntl*$^{LoxP/LoxP}$) and *Arntl*$^{LoxP/LoxP}$*Lyz2*^{Cre} mice. These results demonstrate that BMAL1 regulates the rhythmic oscillations of Ly6C^{hi} monocyte numbers in all three monocyte reservoirs.

We next tested whether disruption of the diurnal rhythms of Ly6C^{hi} monocytes alters their trafficking patterns. Unlike the diurnal recruitment of Ly6C^{hi} monocytes in *Arntl*$^{LoxP/LoxP}$ mice, the inflamed peritoneum of *Arntl*$^{LoxP/LoxP}$*Lyz2*^{Cre} mice had higher numbers of Ly6C^{hi} monocytes, which lacked rhythmicity (fig. S8A). These changes were specific for Ly6C^{hi} monocytes because recruitment of total monocytes did not exhibit a diurnal pattern

(fig. S8B). Moreover, there were no significant differences between the genotypes in the numbers of total monocytes, Ly6C^{hi} monocytes, neutrophils or macrophages in the uninflamed peritoneum (fig. S8C-F). The increased recruitment of Ly6C^{hi} monocytes, however, did amplify the local inflammatory response in *Arntl*$^{LoxP/LoxP}$*Lyz2*^{Cre} mice, as quantified by the release of CCL2, CCL8, IL1β, and IL6 (fig. S9A-D). This increase in peritoneal inflammation was again independent of diurnal changes in the expression of *Il1b* and *Il6* (fig. S9E-F).

The amplification of inflammation in *Arntl*$^{LoxP/LoxP}$*Lyz2*^{Cre} mice suggested that these animals might be predisposed to developing infection-induced systemic inflammation. To test this hypothesis, we infected *Arntl*$^{LoxP/LoxP}$ and *Arntl*$^{LoxP/LoxP}$*Lyz2*^{Cre} mice at ZT0 and ZT8 with non-lethal dose of *L. monocytogenes* and monitored their survival. Compared to *Arntl*$^{LoxP/LoxP}$ mice, all *Arntl*$^{LoxP/LoxP}$*Lyz2*^{Cre} mice exhibited greatly reduced survival with median survival time of 77-91 hours (Fig. 3E), which could not be accounted for by differences in expression of *Tlr2* or *Tlr5* (fig. S9G-H), two pattern recognition receptors that have been implicated in the recognition of *L. monocytogenes* (24, 25). However, *Arntl*$^{LoxP/LoxP}$*Lyz2*^{Cre} mice infected at ZT8 were slightly more susceptible to infection-induced lethality than those infected at ZT0 (Fig. 3E), perhaps reflecting incomplete depletion of BMAL1 protein in the newly recruited bone marrow monocytes (18).

Analysis of sera 2 dpi confirmed that *Arntl*$^{LoxP/LoxP}$*Lyz2*^{Cre} mice had higher circulating concentration of inflammatory cytokines and chemokines, including IL1β, IL6, IFNγ, and CCL2 (Fig. 3F-I). This increase in systemic inflammation occurred in the absence of worsening infection because bacterial CFUs in the spleens and livers of *Arntl*$^{LoxP/LoxP}$*Lyz2*^{Cre} mice were lower or unchanged, respectively (fig. S10A, B), whereas those in peritoneum were marginally higher (fig. S10C). Congruent with the CFU data, spleens rather than livers of *Arntl*$^{LoxP/LoxP}$*Lyz2*^{Cre} mice exhibited a more robust increase in numbers of Tip-DCs, and IFNγ-producing CD4^{+} and CD8^{+} T cells (fig. S10D-K). These data show that BMAL1-dependent diurnal rhythms of Ly6C^{hi} monocytes confers a survival advantage during an infectious challenge with *L. monocytogenes*.

BMAL1 recruits PRC2 complex to repress chemokine genes

The recruitment of Ly6C^{hi} monocytes to inflammatory sites is mediated by the chemokine receptor CCR2 and its ligands, such as CCL2 and CCL8 (26). We observed that expression of CCL2, CCL8, and S100A8, a small calcium binding protein implicated in monocyte chemotaxis (27), is regulated in a diurnal manner in monocytes recruited to sites of inflammation (fig. S11A-C). These observations led to us to ask whether BMAL1/CLOCK heterodimers might directly regulate chemokine gene expression in monocytes and macrophages. Indeed, deletion of *Arntl* resulted in higher expression of all three chemokine genes (*Ccl2, Ccl8*, and *S100a8*) in monocytes and peritoneal macrophages (Fig. 4A, fig. S12A-E), which contributed to increased concentrations of CCL2 and CCL8 in the serum (fig. S12F-G). These data suggest that repression by BMAL1 is necessary to generate diurnal rhythms in chemokine expression. Furthermore, bioinformatic analyses confirmed that promoter regions of *Ccl2, Ccl8*, and *S100a8* contained E-box motifs to which both BMAL1 and CLOCK were recruited in a rhythmic manner (Fig. 4B, and figs. S13A-E). This rhythmic recruitment of BMAL1 or CLOCK to the chemokine promoters was absent in bone marrow-derived macrophages (BMDMs) lacking BMAL1 (Fig. 4B, and figs. S13A-E,), suggesting that BMAL1/CLOCK heterodimers might recruit a repressor complex to silence chemokine gene expression.

Previous studies have demonstrated that histone acetylation and methylation is important in circadian gene expression (28, 29). Amongst the epigenetic marks that regulate clock-controlled genes (CCGs), trimethylation of histone H3 at lysine 27 (H3K27Me3) by

polycomb repressive complex 2 (PRC2) has been implicated in the silencing of CCGs (30), prompting us to ask whether BMAL1 can interact with members of PRC2 in BMDMs. Immunoprecipitation of endogenous BMAL1 not only pulled down CLOCK but also members of PRC2, including the histone methyltransferase EZH2 (enhancer of zeste), EED (extra-sex comb), and SUZ12 (suppressor of zeste) (Fig. 4C). This interaction was specific because we failed to pull down CLOCK or members of PRC2 in BMAL1 deficient BMDMs (Fig. 4C). Chromatin immunoprecipitation experiments revealed that EZH2 was rhythmically recruited to the proximal promoter of *Ccl2* gene in a BMAL1-dependent manner (Fig. 4D), which temporally coincided with its silencing by H3K27Me3 (Fig. 4E). Moreover, in the absence of BMAL1, the chromatin state of the *Ccl2* gene was more active, as evidenced by the presence of H3K4Me3 activation marks and the constitutive recruitment of RNA polymerase II to the promoter (Fig. 4F, G). Similar patterns of EZH2 and RNA polymerase II (Pol II) recruitment, and the associated chromatin modifications were observed on *Ccl8* (fig. S14A-D) and *S100a8* promoters (fig. S15A-D).

We next tested the importance of the CCL2-CCR2 chemokine axis in the maintenance of Ly6C^{hi} diurnal rhythms. Consistent with published reports, the number of total and Ly6C^{hi} monocytes were lower in blood and spleens of *Ccr2*$^{-/-}$ mice (Fig. 4H and fig. S16A-C) (31). Loss of CCR2, however, also abolished the diurnal variation of total and Ly6C^{hi} monocytes in the blood and spleen (Fig. 4H and fig. S16A-C). Because bone marrow monocyte content is anti-phasic to that of the periphery, *Ccr2*$^{-/-}$ mice had a higher number of Ly6C^{hi} monocytes throughout the time course (fig. S16D). In contrast, administration of CCL2 to C57BL/6J mice was sufficient to disrupt the diurnal oscillations of Ly6C^{hi} and total monocytes in all three reservoirs (Fig. 4H and fig. S16A-D). These data indicate that the rhythmic recruitment of the PRC2 complex by BMAL1/CLOCK heterodimers imparts diurnal variation to chemokine expression that is necessary to sustain Ly6C^{hi} monocyte rhythms.

Myeloid cell BMAL1 deficiency worsens metabolic disease

Having established a physiological role for the diurnal rhythms of Ly6C^{hi} monocytes during acute infection, we investigated whether their disruption contributes to pathogenesis of chronic inflammatory diseases. Our initial studies focused on diet-induced obesity and insulin resistance because low-grade chronic inflammation has been shown to modulate the expression of these disease phenotypes (32, 33). We thus fed *Arntl*$^{LoxP/LoxP}$ and *Arntl*$^{LoxP/LoxP}$*Lyz2*^{Cre} mice high fat diet (HFD) for one week and monitored the recruitment of Ly6C^{hi} monocytes to metabolic tissues. Compared to *Arntl*$^{LoxP/LoxP}$ mice, short term HFD feeding induced Ly6C^{hi} monocytosis, and increased the Ly6C^{hi} macrophage content of epididymal white adipose tissue (eWAT) and brown adipose tissue (BAT) of *Arntl*$^{LoxP/LoxP}$*Lyz2*^{Cre} mice (fig. S17A-C). Moreover, in *Arntl*$^{LoxP/LoxP}$*Lyz2*^{Cre} mice, the newly recruited Ly6C^{hi} eWAT and BAT macrophages expressed higher levels of monocyte-attracting chemokines (fig. S17D-F), suggesting that disruption of the diurnal rhythms of monocytes might potentiate metabolic inflammation and disease.

To explore this hypothesis, we fed *Arntl*$^{LoxP/LoxP}$ and *Arntl*$^{LoxP/LoxP}$*Lyz2*^{Cre} mice a HFD and monitored the development of metabolic disease. Compared to *Arntl*$^{LoxP/LoxP}$ mice, *Arntl*$^{LoxP/LoxP}$*Lyz2*^{Cre} mice gained ~30% more weight on HFD, which contributed to their higher total body adiposity and increased tissue weight (Fig. 5A-C). This increase in weight gain likely resulted from a decrease in energy expenditure, as reflected in the lower oxygen consumption rate (~12%) of *Arntl*$^{LoxP/LoxP}$*Lyz2*^{Cre} mice during the day cycle (Fig. 5D). Food intake, total activity, and substrate utilization were not different between *Arntl*$^{LoxP/LoxP}$ and *Arntl*$^{LoxP/LoxP}$*Lyz2*^{Cre} mice (fig. S18A-C).

We next investigated whether chronic exposure to HFD exacerbated inflammation in metabolic tissues of *Arntl*$^{LoxP/LoxP}$*Lyz2*^{Cre} mice. Flow cytometric analysis revealed that *Arntl*$^{LoxP/LoxP}$*Lyz2*^{Cre} mice had higher numbers of total and Ly6C^{hi} (~2.5-fold and ~1.8-fold higher than *Arntl*$^{LoxP/LoxP}$ mice, respectively) macrophages in their eWAT (Fig. 5E, fig. S19A). Macrophage subset analysis further showed that absolute numbers of CD11c^{+} and CD301^{+} macrophages were both higher in eWAT of *Arntl*$^{LoxP/LoxP}$*Lyz2*^{Cre} mice (fig. S19A, B). These inflammatory changes were not restricted to eWAT because we observed similar increases in macrophage content of BAT in *Arntl*$^{LoxP/LoxP}$*Lyz2*^{Cre} mice (fig. S19C, D). Congruent with these observations, there was evidence for increased local and systemic inflammation in *Arntl*$^{LoxP/LoxP}$*Lyz2*^{Cre} mice (fig. S20A-C), including increased infiltration of eWAT and BAT by adaptive immune cells (fig. S20D, E) and higher expression of monocyte-attracting chemokines (fig. S20F-H). In contrast, body weight and macrophage content of eWAT and BAT were not significantly different in mice fed normal chow (fig. S21A-C). These data demonstrate that deletion of *Arntl* in myeloid cells prevents diurnal oscillations between Ly6C^{hi} and Ly6C^{low} monocytes, which potentiates the inflammatory response to obesity.

On the basis of these findings, we assessed whether *Arntl*$^{LoxP/LoxP}$*Lyz2*^{Cre} mice were more prone to developing obesity-associated insulin resistance and metabolic disease. Glucose tolerance testing showed impaired clearance of glucose in *Arntl*$^{LoxP/LoxP}$*Lyz2*^{Cre} mice (Fig. 5F), which likely resulted from a decrease in systemic insulin action (Fig. 5G). Congruent with this postulate, insulin-induced serine phosphorylation of AKT was markedly impaired in eWAT, liver, and skeletal muscles of *Arntl*$^{LoxP/LoxP}$*Lyz2*^{Cre} mice (Fig. 5H, and fig S22A, B). In addition, histological analysis demonstrated ectopic deposition of triglycerides in liver and BAT (fig. S22C-F), and leukocytic infiltration in eWAT (fig. S22G), thus providing further evidence for worsening insulin resistance and metabolic dysfunction in *Arntl*$^{LoxP/LoxP}$*Lyz2*^{Cre} mice.

Because previous studies have demonstrated that changes in feeding period can entrain the peripheral cellular clocks (34), we finally investigated whether monocyte diurnal rhythms are responsive to changes in nutrient intake. As expected, restricting feeding to the daytime induced 12-hour phase shift in liver diurnal gene expression (fig. S23A, B), whereas the expression of clock genes in peritoneal macrophages remained unchanged (fig. S23C, D). Accordingly, the diurnal oscillations of Ly6C^{hi} and total monocytes in all three reservoirs displayed similar rhythms irrespective of the feeding regimen (fig. S23E to I), suggesting that Ly6C^{hi} monocyte rhythms primarily fortify host defenses against anticipatory changes in the environment.

Discussion

Previous studies have demonstrated bidirectional crosstalk between circadian clocks and metabolism (1, 2, 28). For instance, the peripheral clocks in metabolic tissues anticipate feeding-fasting cycles, and conversely, feeding rhythms are strong Zeitgebers that can entrain peripheral clocks of metabolic tissues. In contrast, we found that the diurnal rhythms of myeloid cells do not anticipate metabolic rhythms and cannot be entrained by time restricted feeding cycles. This suggests that the primary function of diurnal oscillations in myeloid cell numbers is not in anticipatory regulation of metabolism but perhaps in host defense. In support of this idea, both the time of infection and myeloid-specific BMAL1 are critical determinants of the pathology associated with infectious challenge with *L. monocytogenes*. Moreover, the ability of CCL2, whose expression is induced upon sensing of pathogens, to override the diurnal oscillations in myeloid cell numbers provides a mechanism by which the host defenses can shift from anticipatory to pathogen-directed responses.

Although diurnal variations in monocyte numbers is not entrained by feeding cues, its disruption does render mice susceptible to diet-induced obesity and insulin resistance. The increased susceptibility of $Arntl^{LoxP/LoxP}Lyz2^{Cre}$ mice to metabolic disease likely results from $Ly6C^{hi}$ monocytosis, and the subsequent recruitment of these cells into metabolically stressed adipose tissue. This potentiates the chronic inflammatory response both locally and systemically, resulting in insulin resistance and hyperglycemia. Finally, since chronic inflammatory diseases, such as myocardial infarction, asthma, and rheumatoid arthritis, exhibit diurnal clustering in humans (35-37), rhythmic oscillations of inflammatory monocytes might also contribute to their pathogenesis.

Supplementary Material

Refer to Web version on PubMed Central for supplementary material.

Acknowledgments

We thank members of the Chawla laboratory and A. Loh for comments on the manuscript. The data presented in this paper are tabulated in the main paper and in the supplementary materials. The authors' work was supported by grants from NIH (HL076746, DK094641), Larry L. Hillblom Foundation Network Grant, Diabetes Family Fund (University of California, San Francisco), and an NIH Director's Pioneer Award (DP1AR064158) to A.C.; and NIH (PO1AI063302) to J.S.C. K.D.N. was supported by Stanford Graduate and AHA Predoctoral Fellowships, Y.Q. by AHA Postdoctoral Fellowship, and S.J.F. by NIH Training Grant (T32AI007334). All animal care and procedures were performed in accordance with Stanford University's A-PLAC and UCSF's IACUC guidelines.

REFERENCES AND NOTES

1. Asher G, Schibler U. Crosstalk between components of circadian and metabolic cycles in mammals. Cell Metab. Feb 2.2011 13:125. [PubMed: 21284980]
2. Bass J, Takahashi JS. Circadian integration of metabolism and energetics. Science. Dec 3.2010 330:1349. [PubMed: 21127246]
3. Saini C, Suter DM, Liani A, Gos P, Schibler U. The mammalian circadian timing system: synchronization of peripheral clocks. Cold Spring Harb Symp Quant Biol. 2011; 76:39. [PubMed: 22179985]
4. Gibbs JE, et al. The nuclear receptor REV-ERBalpha mediates circadian regulation of innate immunity through selective regulation of inflammatory cytokines. Proc Natl Acad Sci U S A. Jan 10.2012 109:582. [PubMed: 22184247]
5. Keller M, et al. A circadian clock in macrophages controls inflammatory immune responses. Proc Natl Acad Sci U S A. Dec 15.2009 106:21407. [PubMed: 19955445]
6. Scheiermann C, Kunisaki Y, Frenette PS. Circadian control of the immune system. Nat Rev Immunol. Mar.2013 13:190. [PubMed: 23391992]
7. Haus E, Smolensky MH. Biologic rhythms in the immune system. Chronobiology international. Sep.1999 16:581. [PubMed: 10513884]
8. Scheiermann C, et al. Adrenergic nerves govern circadian leukocyte recruitment to tissues. Immunity. Aug 24.2012 37:290. [PubMed: 22863835]
9. Hayashi M, Shimba S, Tezuka M. Characterization of the molecular clock in mouse peritoneal macrophages. Biological & pharmaceutical bulletin. Apr.2007 30:621. [PubMed: 17409491]
10. Geissmann F, et al. Development of monocytes, macrophages, and dendritic cells. Science. Feb 5.2010 327:656. [PubMed: 20133564]
11. Medzhitov R. Origin and physiological roles of inflammation. Nature. Jul 24.2008 454:428. [PubMed: 18650913]
12. Yoo SH, et al. PERIOD2::LUCIFERASE real-time reporting of circadian dynamics reveals persistent circadian oscillations in mouse peripheral tissues. Proc Natl Acad Sci U S A. Apr 13.2004 101:5339. [PubMed: 14963227]
13. Auffray C, et al. Monitoring of blood vessels and tissues by a population of monocytes with patrolling behavior. Science. Aug 3.2007 317:666. [PubMed: 17673663]

14. Geissmann F, Jung S, Littman DR. Blood monocytes consist of two principal subsets with distinct migratory properties. Immunity. Jul.2003 19:71. [PubMed: 12871640]
15. Boring L, et al. Impaired monocyte migration and reduced type 1 (Th1) cytokine responses in C-C chemokine receptor 2 knockout mice. J Clin Invest. Nov 15.1997 100:2552. [PubMed: 9366570]
16. Robbins CS, Swirski FK. The multiple roles of monocyte subsets in steady state and inflammation. Cellular and molecular life sciences : CMLS. Aug.2010 67:2685. [PubMed: 20437077]
17. Materials and methods are available as supporting material on Science Online.
18. Serbina NV, Shi C, Pamer EG. Monocyte-mediated immune defense against murine Listeria monocytogenes infection. Advances in immunology. 2012; 113:119. [PubMed: 22244581]
19. Serbina NV, Salazar-Mather TP, Biron CA, Kuziel WA, Pamer EG. TNF/iNOS-producing dendritic cells mediate innate immune defense against bacterial infection. Immunity. Jul.2003 19:59. [PubMed: 12871639]
20. Shi C, et al. Ly6G+ neutrophils are dispensable for defense against systemic Listeria monocytogenes infection. J Immunol. Nov 15.2011 187:5293. [PubMed: 21976773]
21. Silver AC, Arjona A, Walker WE, Fikrig E. The circadian clock controls toll-like receptor 9-mediated innate and adaptive immunity. Immunity. Feb 24.2012 36:251. [PubMed: 22342842]
22. Shackelford PG, Feigin RD. Periodicity of susceptibility to pneumococcal infection: influence of light and adrenocortical secretions. Science. Oct 19.1973 182:285. [PubMed: 4147530]
23. Lamia KA, Storch KF, Weitz CJ. Physiological significance of a peripheral tissue circadian clock. Proc Natl Acad Sci U S A. Sep 30.2008 105:15172. [PubMed: 18779586]
24. Hayashi F, et al. The innate immune response to bacterial flagellin is mediated by Toll-like receptor 5. Nature. Apr 26.2001 410:1099. [PubMed: 11323673]
25. Torres D, et al. Toll-like receptor 2 is required for optimal control of Listeria monocytogenes infection. Infection and immunity. Apr.2004 72:2131. [PubMed: 15039335]
26. Shi C, Pamer EG. Monocyte recruitment during infection and inflammation. Nat Rev Immunol. Nov.2011 11:762. [PubMed: 21984070]
27. Cornish CJ, et al. S100 protein CP-10 stimulates myeloid cell chemotaxis without activation. Journal of cellular physiology. Feb.1996 166:427. [PubMed: 8592003]
28. Feng D, Lazar MA. Clocks, metabolism, and the epigenome. Molecular cell. Jul 27.2012 47:158. [PubMed: 22841001]
29. Sahar S, Sassone-Corsi P. The epigenetic language of circadian clocks. Handbook of experimental pharmacology. 2013; 217:29. [PubMed: 23604474]
30. Etchegaray JP, et al. The polycomb group protein EZH2 is required for mammalian circadian clock function. J Biol Chem. Jul 28.2006 281:21209. [PubMed: 16717091]
31. Tsou CL, et al. Critical roles for CCR2 and MCP-3 in monocyte mobilization from bone marrow and recruitment to inflammatory sites. J Clin Invest. Apr.2007 117:902. [PubMed: 17364026]
32. Hotamisligil GS. Inflammation and metabolic disorders. Nature. 2006; 444:860. 2006/12/14/print. [PubMed: 17167474]
33. Odegaard JI, Chawla A. Pleiotropic actions of insulin resistance and inflammation in metabolic homeostasis. Science. Jan 11.2013 339:172. [PubMed: 23307735]
34. Damiola F, et al. Restricted feeding uncouples circadian oscillators in peripheral tissues from the central pacemaker in the suprachiasmatic nucleus. Genes & development. Dec 1.2000 14:2950. [PubMed: 11114885]
35. Martin RJ. Nocturnal asthma: circadian rhythms and therapeutic interventions. The American review of respiratory disease. Jun.1993 147:S25. [PubMed: 8494197]
36. Muller JE, et al. Circadian variation in the frequency of onset of acute myocardial infarction. The New England journal of medicine. Nov 21.1985 313:1315. [PubMed: 2865677]
37. Straub RH, Cutolo M. Circadian rhythms in rheumatoid arthritis: implications for pathophysiology and therapeutic management. Arthritis Rheum. Feb.2007 56:399. [PubMed: 17265475]
38. Nagoshi E, et al. Circadian gene expression in individual fibroblasts: cell-autonomous and self-sustained oscillators pass time to daughter cells. Cell. Nov 24.2004 119:693. [PubMed: 15550250]
39. Lieberman LA, Higgins DE. Inhibition of Listeria monocytogenes infection by neurological drugs. International journal of antimicrobial agents. Mar.2010 35:292. [PubMed: 20031379]

40. Nguyen KD, et al. Alternatively activated macrophages produce catecholamines to sustain adaptive thermogenesis. Nature. Dec 1.2011 480:104. [PubMed: 22101429]

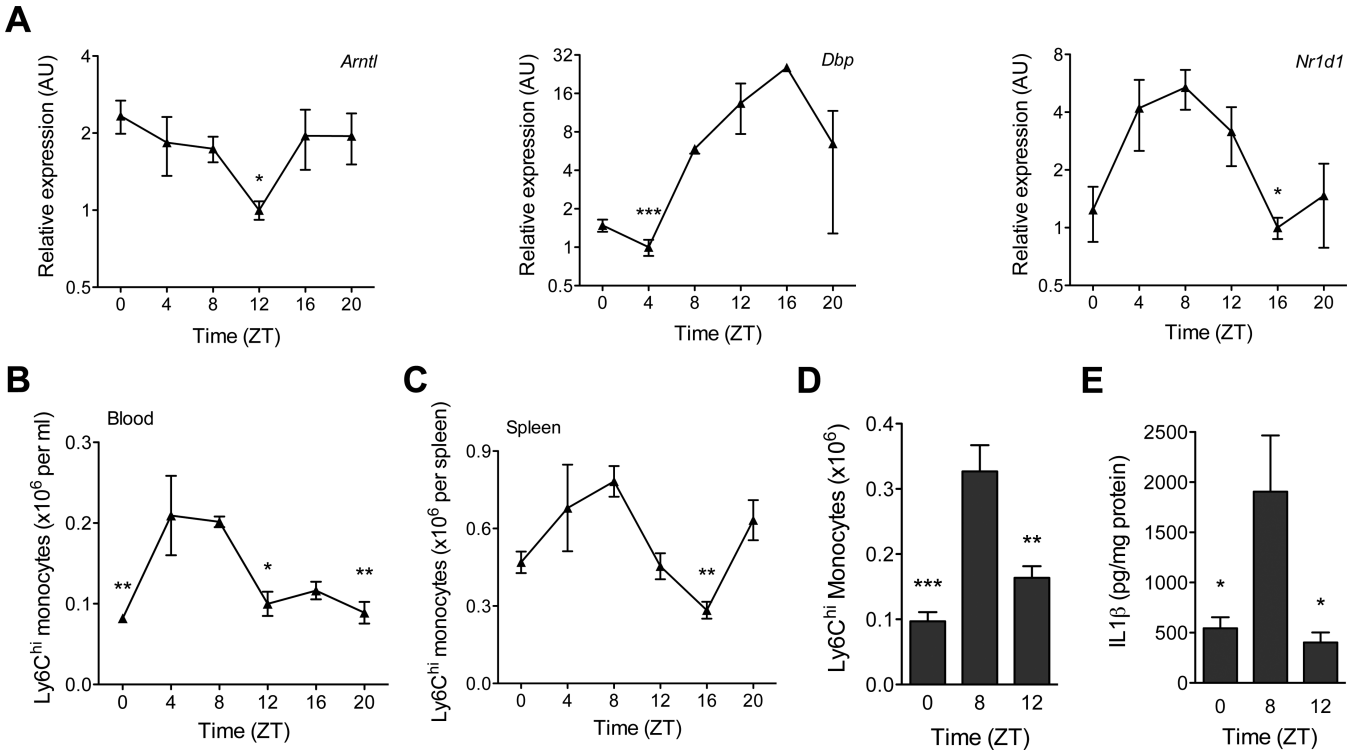

Fig. 1. Diurnal variation of Ly6C^{hi} monocytes

(**A**) Quantitative RT-PCR analysis of clock controlled genes (*Arntl, Nr1d1*, and *Dbp*) in blood monocytes during a 12 hour light-dark cycle (n = 3-4 samples per time point). (**B** and **C**) Ly6C^{hi} monocyte numbers in blood (B) and spleen (C) during a 12 hour light-dark cycle (n=5 mice per time point). (**D** and **E**) Recruitment of Ly6C^{hi} monocytes to inflamed peritoneum. Ly6C^{hi} monocyte number (D), and concentration of IL1β (E) were quantified in the peritoneal fluid 2 hours after elicitation with thioglycollate (n = 5 mice per time point). Pooled data (A) or representatives (B to E) of two independent experiments are shown as mean ± SEM. Two-tailed Student's t-tests (A) and one-way ANOVA (B-E) are used for statistical analyses (comparisons were made between the acrophase and other time points). *P<0.05; **P<0.01; ***P<0.001.

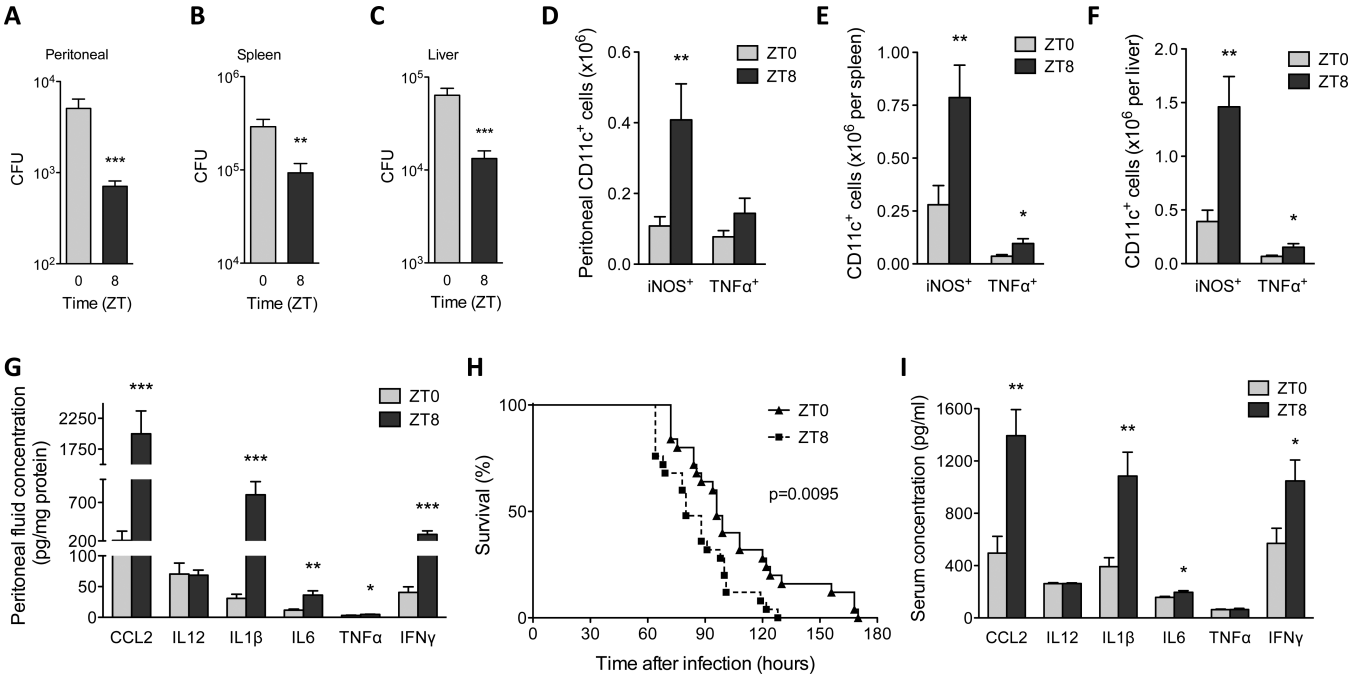

Fig. 2. Diurnal variation in the pathogenicity of *Listeria monocytogenes*

(**A** to **C**) Mice kept under a 12 hour light-dark cycle were intraperitoneally inoculated with 1×10^6 *L. monocytogenes* at ZT0 and ZT8, and colony forming units (CFUs) recovered from the peritoneal cavity (A), spleen (B), and liver (C) were quantified 2 dpi (n = 14-15 mice per time point). (**D** to **F**) Numbers of $iNOS^+CD11c^+$ and $TNF\alpha^+CD11c^+$ cells in peritoneal cavity (D), spleen (E), and liver (F) of mice 2 dpi with 1×10^6 *L. monocytogenes* at ZT0 and ZT8 (n = 15 mice per time point). (**G**) Concentration of chemokines and cytokines in peritoneal fluid 2 dpi with 1×10^6 *L. monocytogenes* at ZT0 and ZT8 (n = 15 mice per time point). (**H**) Survival curves of mice after infection with 1×10^7 *L. monocytogenes* at ZT0 and ZT8 (n = 25 mice per time point). (**I**) Serum concentration of chemokines and cytokines 2 dpi with 1×10^7 *L. monocytogenes* at ZT0 and ZT8 (n = 10 mice per time point). Pooled data from two or three independent experiments are presented as mean ± SEM. Statistical significance (*P<0.05; **P < 0.01; ***P < 0.001) was assessed using two-tailed Student's *t*-test (A to G, and I), and log-rank test (H).

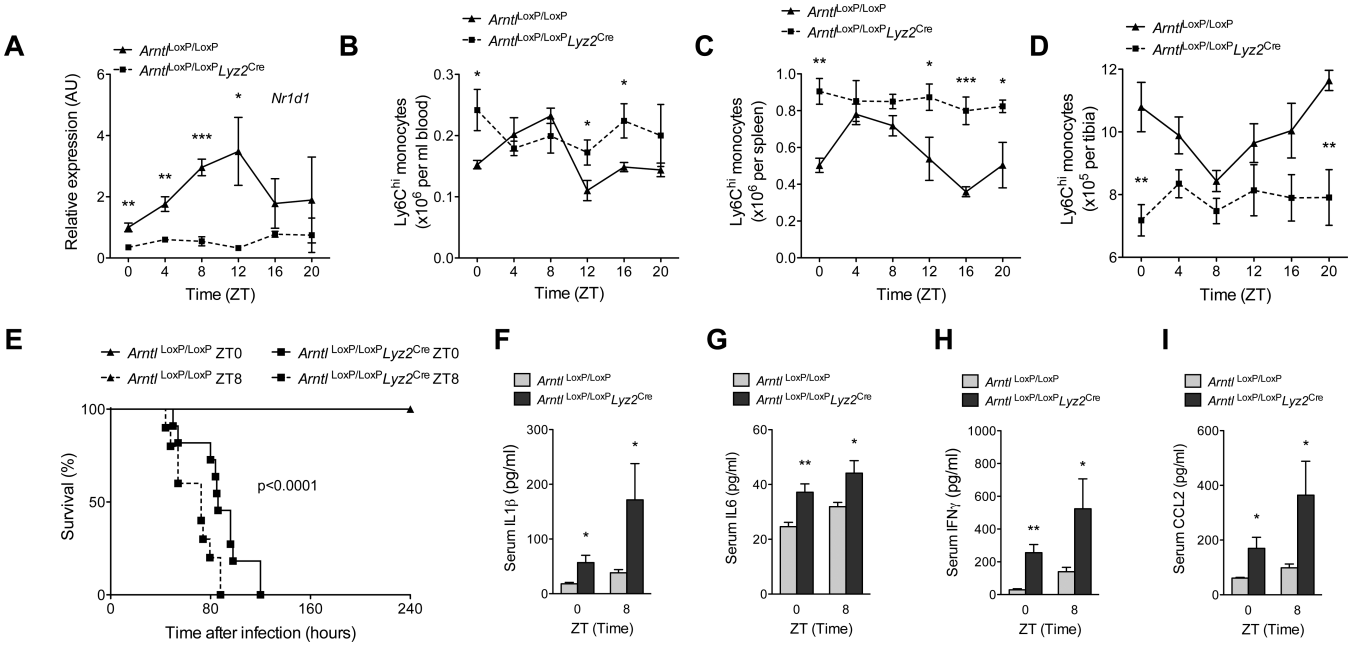

Fig. 3. BMAL1 regulates rhythmic oscillations of Ly6C^{hi} monocytes in a cell autonomous manner

(**A**) Quantitative RT-PCR kinetic analysis of *Nr1d1* mRNA in blood monocytes isolated from *Arntl*$^{LoxP/LoxP}$ and *Arntl*$^{LoxP/LoxP}$*Lyz2*^{Cre} mice kept on a 12 hour light-dark cycle (n = 3-4 samples per genotype and time point). (**B** to **D**) Ly6C^{hi} monocyte numbers in blood (B), spleen (C), and bone marrow (D) of *Arntl*$^{LoxP/LoxP}$ and *Arntl*$^{LoxP/LoxP}$*Lyz2*^{Cre} mice kept under a 12 hour light-dark cycle at various ZTs. (n = 5 mice per genotype and time point). (**E**) Survival curves of *Arntl*$^{LoxP/LoxP}$ and *Arntl*$^{LoxP/LoxP}$*Lyz2*^{Cre} mice after infection with 1×10^6 *L. monocytogenes* at ZT0 and ZT8 (n = mice 10-11 per genotype and time point). (**F** to **I**) Serum concentrations of IL1β (F), IL6 (G), IFNγ (H), and CCL2 (I) in *Arntl*$^{LoxP/LoxP}$ and *Arntl*$^{LoxP/LoxP}$*Lyz2*^{Cre} mice 2 dpi with 1×10^6 *L. monocytogenes* at ZT0 and ZT8 (n = mice 4-6 per genotype and time point). Pooled data (A and E) and representative (B to D) of two to three independent experiments are shown as mean ± SEM and analyzed using two-tailed Student's *t*-tests (A to D, and F to I), and log-rank test (E). **P*<0.05; ***P*<0.01; ****P*<0.001.

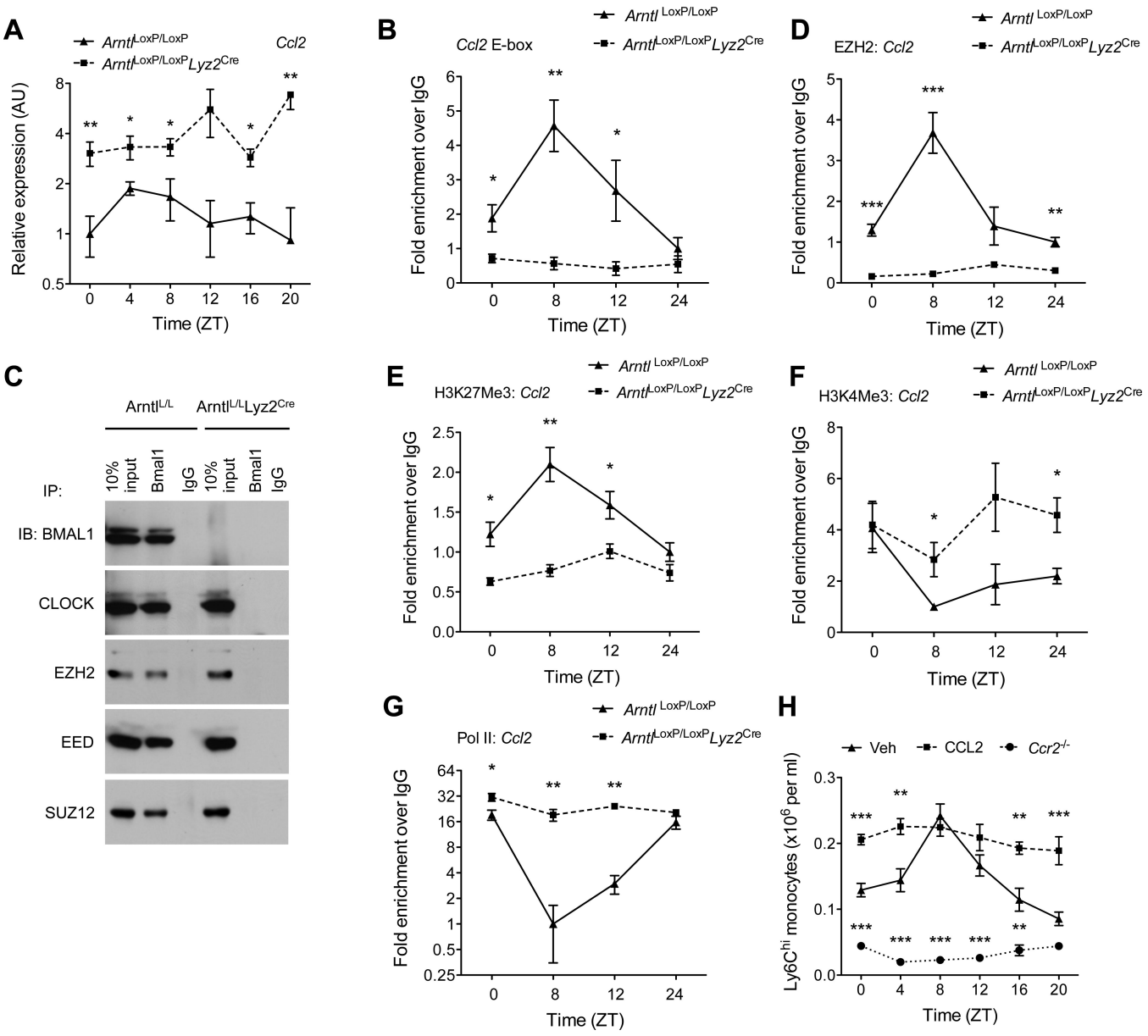

Fig. 4. BMAL1 recruits PRC2 to repress expression of *Ccl2*

(**A**) Quantitative RT-PCR analysis of *Ccl2* expression in blood monocytes of *Arntl*$^{LoxP/LoxP}$ and *Arntl*$^{LoxP/LoxP}$*Lyz2*^{Cre} mice kept on a 12 hour day-ligh cycle (n = 3-4 samples per genotype and time point). (**B**) ChIP analysis of BMAL1 binding to the *Ccl2* promoter (n = 4 samples per genotype and time point). (**C**) Coimmunoprecipitation of BMAL1 and with members of PRC2. Nuclear lysates from serum shocked BMDMs were immunopercipiated with BMAL1 antibody, and immunoblotted for BMAL1, CLOCK, EZH2, EED, and SUZ12. (**D** and **G**) ChIP analysis for the recruitment of EZH2 (D) and Pol II (G) to the proximal promoter of the *Ccl2* gene (n = 4 samples per genotype and time point). (**E** and **F**) ChIP analysis for H3K27Me3 (E) and H3K4Me3 (F) at the proximal promoter of *Ccl2* gene (n = 4 samples per genotype and time point). (**H**) Ly6C^{hi} monocyte numbers in the blood of wild type or *Ccr2*$^{-/-}$ mice during a 12 hour light-dark cycle. Wild type mice were intraperitoneally injected with PBS (Veh) or CCL2 (20 μgkg^{-1}) 24 hours prior to quantification of Ly6C^{hi} monocytes (n = 4-5 mice per genotype/treatment and time point).

Pooled data (A to G) from two independent experiments are shown as mean ± S.E.M and analyzed using two-tailed Student's *t*-tests (A and B; D to G) and two-way ANOVA (H). $*P<0.05$; $**P<0.01$; $***P<0.001$ represent comparison between $Arntl^{LoxP/LoxP}$ and $Arntl^{LoxP/LoxP}Lyz2^{Cre}$ or between wild type treated Veh vs. CCL2 or $Ccr2^{-/-}$ at each time point.

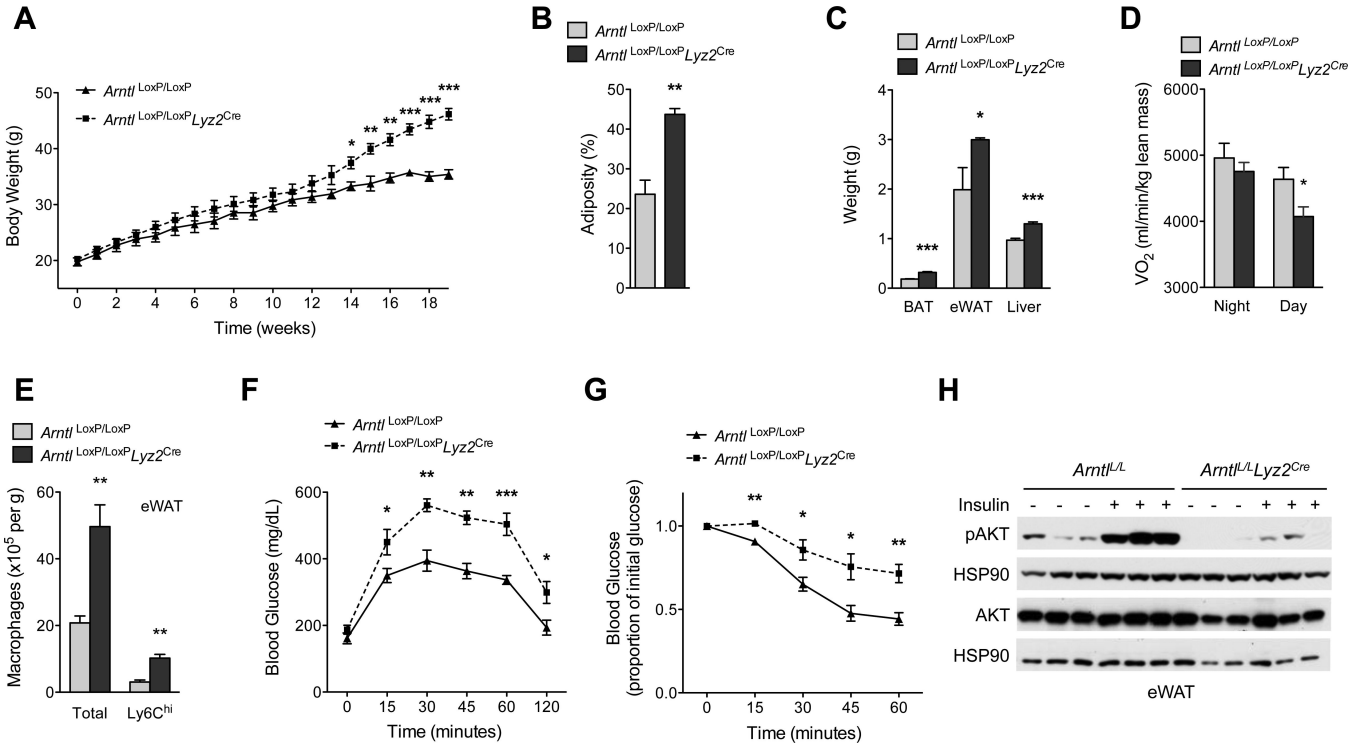

Fig. 5. Myeloid cell-specific deletion of BMAL1 exacerbates metabolic disease

(**A** to **D**) Body weight (A), adiposity (B), tissue weights (C) and oxygen consumption (D) in *Arntl*$^{\text{LoxP/LoxP}}$ and *Arntl*$^{\text{LoxP/LoxP}}$*Lyz2*$^{\text{Cre}}$ mice kept on a 12 hour light-dark cycle fed high fat diet for 19 weeks (n = 4-5 mice per genotype). (**E**) Total and Ly6C$^{\text{hi}}$ macrophage content in eWAT of *Arntl*$^{\text{LoxP/LoxP}}$ and *Arntl*$^{\text{LoxP/LoxP}}$*Lyz2*$^{\text{Cre}}$ mice fed high fat diet (n = 5 mice per genotype). (**F** and **G**) Glucose (F) and insulin tolerance (G) tests of *Arntl*$^{\text{LoxP/LoxP}}$ and *Arntl*$^{\text{LoxP/LoxP}}$*Lyz2*$^{\text{Cre}}$ mice fed high fat diet (n = 5-8 mice per genotype). (**H**) Immunoblots of total and phosphorylated AKT (pAKT) in eWAT of obese *Arntl*$^{\text{LoxP/LoxP}}$ and *Arntl*$^{\text{LoxP/LoxP}}$*Lyz2*$^{\text{Cre}}$ administered intraportal insulin. Representative data of two to four independent experiments (A to C, E to H) are shown as mean ± S.E.M and analyzed using two-tailed Student's *t*-tests. **P*<0.05; ***P*<0.01; ****P*<0.001.